ARTICLE

Grain Growth Kinetics of $BaTiO_3$ Nanocrystals During Calcining Process

Xiao-lan Song[a*], Xi He[a], Hai-ping Yang[a], Yi-xin Qu[b], Guan-zhou Qiu[a]

a. School of Resources Processing and Bioengineering, Central South University, Changsha 410083, China

b. College of Chemical Engineering, Beijing University of Chemical Technology, Beijing 100029, China

(Dated: Received on November 1, 2007; Accepted on March 31, 2008)

$BaTiO_3$ nanocrystals were synthesized by sol-gel method using barium acetate ($Ba(CH_3COO)_2$) and tetrabutyl titanate ($Ti(OC_4H_9)_4$) as raw materials. Xerogel precursors and products were characterized by means of thermogravimetric/differential scanning calorimetry (TG/DSC), X-ray diffraction (XRD) and transmission electron microscope (TEM). The influence of the calcination temperature and duration on the lattice constant, the lattice distortion, and the grain size of $BaTiO_3$ nanocrystals was discussed based on the XRD results. The grain growth kinetics of $BaTiO_3$ nanocrystals during the calcination process were simulated with a conventional grain growth model which only takes into account diffusion, and an isothermal model proposed by Qu and Song, which takes into account both diffusion and surface reactions. Using these models, the pre-exponential factor and the activation energy of the rate constant were estimated. The simulation results indicate that the isothermal model is superior to the conventional one in describing the grain growth process, implying that both diffusion and surface reactions play important roles in the grain growth process.

Key words: $BaTiO_3$ nanocrystal, Sol-gel method, Grain growth kinetics

I. INTRODUCTION

Ferroelectric bulk ceramics have found wide applications in the manufacture of electronic, acousto-optic and piezoelectric devices [1]. Barium titanate ($BaTiO_3$) has become a basic ferroelectric ceramic since the discovery of its high permittivity as a ferroelectric material in 1942 [2]. It is being widely applied in the manufacture of multilayer ceramic capacitors (MLCC), positive temperature coefficient (PTC) electronic ceramics, infrared detectors, thermistors, transducers and electro-optic devices, etc. [3-8]. To prepare ferroelectric $BaTiO_3$ bulk powder and ceramics, various methods such as conventional solid state reaction [9-11], co-precipitation [12-14], hydrothermal [15-17] and sol-gel method [18,19] have been used. Sol-gel method is a preferred technique in the preparation of $BaTiO_3$ with new compositions since there are possibilities to control the stoichiometry and homogeneity of the final products. In addition, it also offers advantages for the production of $BaTiO_3$with fine grain sizes at lower temperature.

Depending on calcination temperature, $BaTiO_3$ can have four crystal forms: rhombohedra, orthorhombic, tetragonal and cubic [20-23]. The electrical properties of $BaTiO_3$ strongly depend on its microstructure as well as chemical composition. A fine grain is essential to achieve optimum dielectric property [24]. Sol-gel method can produce nano-sized crystals. The calcination procedure is important in forming the nano-sized crystals and influences their stability in application. Therefore, a detailed study concerning grain growth kinetics during calcination is necessary to understand the grain growth behavior. In this work, we prepared $BaTiO_3$ using sol-gel method and investigated the influence of calcination conditions on the grain parameters. Based on the experimental results, the grain growth kinetics was simulated using a conventional diffusion model and an isothermal model that takes into account both diffusion and surface reactions.

II. EXPERIMENTS

In this study, $BaTiO_3$ nanocrystal powders were synthesized by sol-gel method. Barium acetate ($Ba(CH_3COO)_2$) and tetrabutyl titanate ($Ti(OC_4H_9)_4$) were used as starting materials, acetic acid (CH_3COOH) and alcohol were used as solvents. $Ba(Ac)_2$ dissolved in acetic acid was mixed with tetrabutyl titanate dissolved in alcohol with vigorous stirring at 40 °C for 1 h to form $BaTiO_3$ precursor. The reactions that occurred in this step can be expressed as:

$$Ti(OC_4H_9)_4 + Ba(Ac)_2 + 3H_2O \rightarrow BaTiO_3 + 4C_4H_{10}O + 2HAc$$

Then it was gelled at room temperature for 48 h. After drying at 80 °C for 6 h, xerogel was obtained. To avoid precipitation, a small amount of glycol was added. Finally the xerogel was calcined at different temperatures to obtain $BaTiO_3$ powder.

The crystallization process of $BaTiO_3$ gel was studied with the aid of DSC/TG (German NETZSCH, STA449C), and XRD (Rigaku D/max-2550VB$^+$ pow-

*Author to whom correspondence should be addressed. E-mail: xlsong@hnu.cn, Tel: +86-731-8830346

der diffractometer). The microstructure of the powders was examined with TEM (H-800 microscope). The grain size of $BaTiO_3$ nanocrystals was calculated using the Scherrer equation with the line-broadening width of (101) face [25].

$$D = 0.89\lambda/B\cos\theta \quad (1)$$

where D is the grain size, B is the line-broadening width, θ is Bragg diffraction angle, and λ is the wave length of X-ray (0.154178 nm).

III. RESULTS AND DISCUSSION

A. Characterization of $BaTiO_3$ nanocrystals

The thermal decomposition process of the $BaTiO_3$ xerogel during calcination in air was studied using DSC/TG. The results are shown in Fig.1. As can be seen from Fig.1, the total weight loss of the xerogel from 30 °C to 1200 °C amounts to 35.1%. The decomposition process can be divided into five stages. The first stage is in the temperature range of 30-110°C. The weight loss is about 7.2%, which can be attributed to the removal of water. In this stage an endothermic peak at about 80 °C on the DSC curve appears. The second stage is in the temperature range of 100-280 °C, the corresponding weight loss is about 2.1%, which can be attributed to the evaporation of organic solvents. On the DSC curve, no significant thermal effect was observed in the second stage. The third stage is in the temperature range of 280-450 °C. The corresponding weight loss is 17.8%, which can be attributed to the combustion of the organic materials of the framework of the xerogel. On the DSC curve, two exothermic peaks at 400 and 450 °C can be observed. The fourth stage is in the temperature range of 450-1040 °C. The corresponding weight loss is 8.1%. On the DSC curve, an exothermic peak at 740 °C and an endothermic peak at 805 °C appear due to the formation of $BaTiO_3$ and a phase transformation. The weight loss in this stage is probably due to the removal of carbon materials. The last stage is in the range of 1040-1200 °C, where no significant change in the weight is observed. However, an exothermic peak on the DSC curve appears, which is probably also due to a phase transformation.

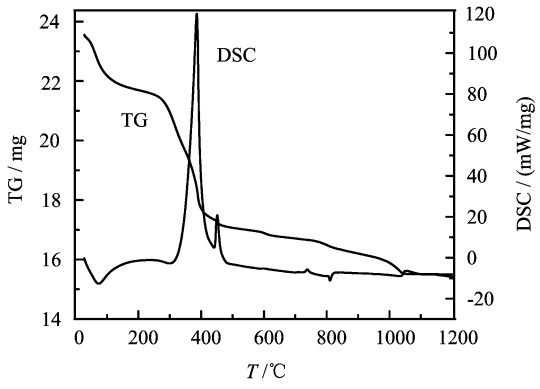

FIG. 1 DSC/TG curves of the $BaTiO_3$ nanocrystal precursor.

XRD patterns of the product powders obtained via calcination at different conditions are shown in Fig.2. With increasing calcination temperature from 700 °C to 1200 °C (duration=2 h) or with increasing calcination duration from 1 h to 5 h ($T = 800$ °C), the main diffraction peaks of $BaTiO_3$ become narrow and sharp. Figure 2(a) indicates that a calcination temperature of 800 °C is not high enough to completely convert $BaCO_3$ into $BaTiO_3$, even if the calcination duration is prolonged to 5 h. Figure 2(b) indicates that upon calcination at 1200 °C for 2 h, the diffraction peaks of $BaCO_3$ disappear. This implies that thermal aging at a temperature of as high as 1200 °C is necessary for the crystallization of $BaTiO_3$ and the complete removal of $BaCO_3$ from the product.

The TEM images of $BaTiO_3$ nanocrystals obtained via calcination at 1000 °C for 2 h are shown in Fig.3. The particles are well-defined crystals with an average size of 30 nm as determined from the images.

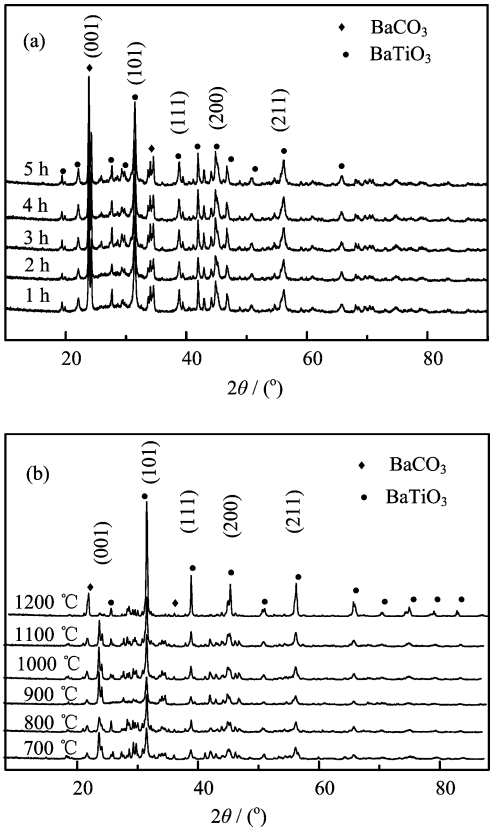

FIG. 2 XRD patterns of $BaTiO_3$ nanocrystals (a) calcined at 800 °C for different durations and (b) calcined at different temperatures for 2 h.

DOI:10.1088/1674-0068/21/03/295-300

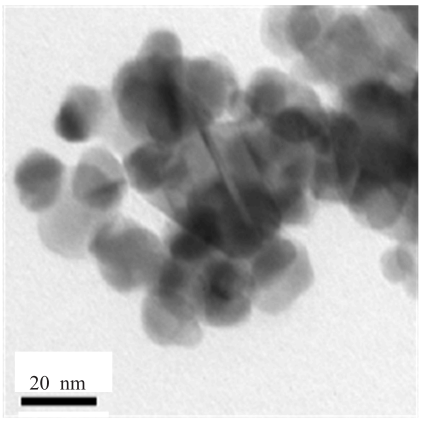

FIG. 3 TEM images of $BaTiO_3$ nanocrystals calcined at 1000 °C for 2 h.

B. Lattice constant and lattice distortion of $BaTiO_3$ nanocrystals

Depending on the calcination temperature, $BaTiO_3$ can have four crystal forms: rhombohedra, orthorhombic, tetragonal and cubic. Above 120 °C, the thermal stable phase is cuboctahedron, its lattice constant (a) can be calculated using the following equation [26],

$$a = \frac{\lambda}{2\sin\theta}\sqrt{h^2+k^2+l^2} \tag{2}$$

where h, k, l are the indices of the crystallographic plane. In this study, the (101) plane of the cubocahedron $BaTiO_3$ is used to calculate the values of a. The effect of calcination temperature and calcination duration on the values of a is investigated. Results show that calcination temperature and duration do not have a significant influence on the lattice constant of $BaTiO_3$. This implies that the lattice constant of cubocahedron $BaTiO_3$ can be regarded as constant during calcination.

Grain recapitalization and lattice distortion are reflected by diffraction half-peak-breadth broadening in XRD patterns. The average lattice distortion of $BaTiO_3$ nanocrystals vertical to the (101) plane can be estimated using the following equation [27],

$$(2\omega)^2\cos^2\theta = \frac{4}{\pi^2}\left(\frac{\lambda}{D_{(hkl)}}\right)^2 + 32\varepsilon^2\sin^2\theta \tag{3}$$

where ε is the average lattice distortion degree vertical to (h k l) plane, $D_{(hkl)}$ is the average particle size, and 2ω is the half-peak-breadth after instrument correction.

The estimated lattice distortion degree of $BaTiO_3$ nanocrystals obtained at different calcination temperatures and durations are shown in Fig.4. Increasing the calcination temperature and duration results in a reduction of the lattice distortion degree of $BaTiO_3$ nanocrystals.

Upon calcination of the xerogel, $BaTiO_3$ nanocrystals are formed via solid phase reactions. At low temperatures, the growth of the crystal nucleus is difficult due to the slow diffusion of particles. As a consequence, crystal grains are small and there are a lot of defects on the crystalline planes. The lattice distortion is larger as well. At this stage, the grains have a larger specific surface area and a higher specific surface energy. Therefore, such powder has higher surface activity. As the calcination temperature increases, the grains grow, and their structure becomes regulated, which is driven by the dynamic force of the surface energy. At a high enough temperature, larger grains are formed with an almost perfect structure showing a small degree of lattice distortion.

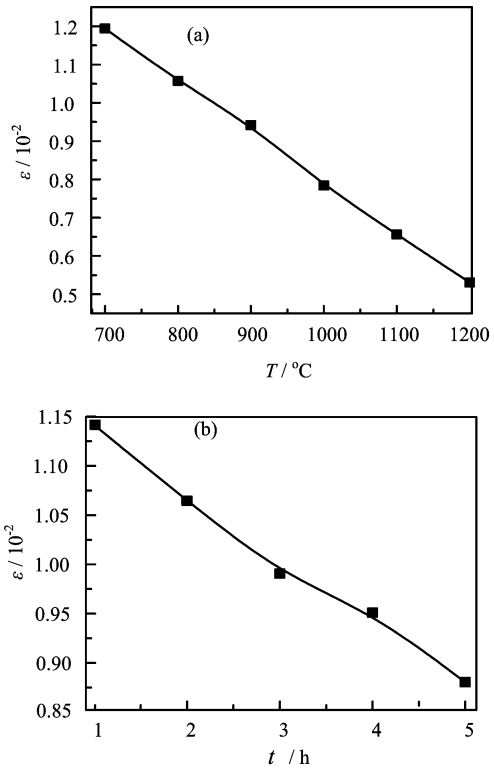

FIG. 4 (a) Effect of calcination temperature on the lattice distortion degree of $BaTiO_3$ nanocrystals calcined for 2 h and (b) effect of calcination duration on the lattice distortion degree of $BaTiO_3$ nanocrystals calcined at 800 °C.

C. Grain growth kinetics of $BaTiO_3$ nanocrystals

The influence of the calcination temperature and duration on the grain size calculated using Eq.(1) is shown in Fig.5. For a calcination duration of 2 h, the grain size increases from 24 nm to 55 nm as the temperature increases from 700 °C to 1200 °C. At 800 °C, the grain size increases from 25 nm to 32 nm as the calcination duration increases from 1 h to 5 h.

In the conventional polycrystalline model, grain growth is proposed to be controlled by atomic diffusion at the grain boundary. The grain growth rate is proportional to the radius of the curvature of the grain.

DOI:10.1088/1674-0068/21/03/295-300

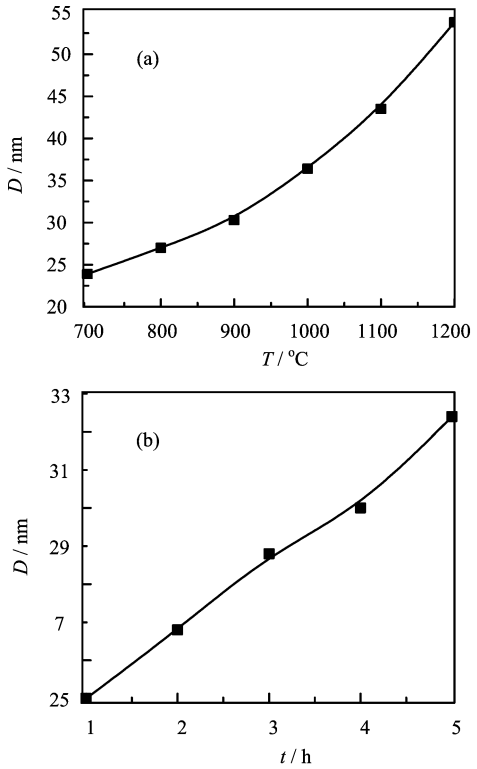

FIG. 5 Variation of grain size of $BaTiO_3$ nanocrystal with calcination temperature and calcination duration. (a) $BaTiO_3$ nanocrystal was calcined at different temperatures for 2 h. (b) $BaTiO_3$ nanocrystal was calcined at 800 °C for different durations.

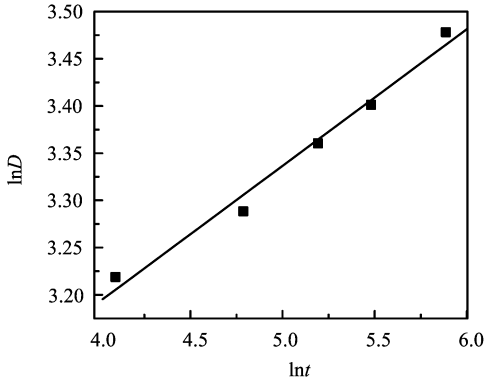

FIG. 6 Linear relationship between ln$D$ and ln$t$.

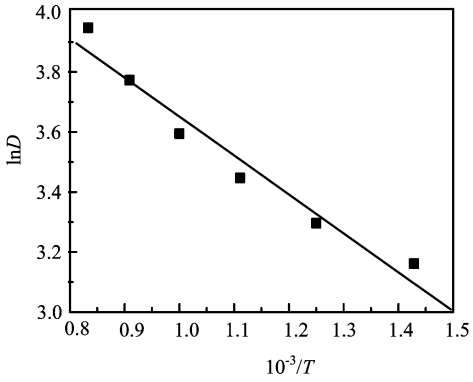

FIG. 7 Linear relationship between ln$D$ and $1/T$.

The grain growth kinetics can be described as [28],

$$D^n - D_0^n = kt \tag{4}$$

where D is the average grain size after annealing, D_0 is the initial grain size, k is the temperature-dependent rate constant, and n is the grain growth exponential reflecting grain growth behavior. Constant k can be expressed by the Arrhenius equation, k=Aexp($-E/RT$) with A being the pre-exponential factor, E being the activation energy, and R being the universal gas constant. Since D_0 is generally much smaller that D, Eq.(4) can be rearranged as:

$$\ln D = \frac{1}{n}\left[\ln t + \ln A - \frac{E}{RT}\right] \tag{5}$$

Eq.(5) indicates that at a fixed calcination temperature, there is a linear relationship between ln$D$ and ln$t$. For a fixed calcination duration, there is a linear relationship between ln$D$ and $1/T$. The ln$D$ values of $BaTiO_3$ nanocrystals calcined at 800 °C as a function of ln$t$ are shown in Fig.6. The value of n obtained by regression using the least squares method is 7. With n=7, for a calcination duration of 2 h, the ln$D$ values of $BaTiO_3$ nanocrystals calcined at temperatures from 800 °C to 1200 °C as a function of $1/T$ are shown in Fig.7. The value of E obtained by regression using the least squares method is 75.49 kJ/mol.

In the conventional model, the driving force for the grain growth is regarded as due to the tendency of the reduction in the total grain boundary energy. However, for nanocrystal materials, the grain growth kinetics cannot be satisfactorily simulated using the conventional model. Qu and song proposed that during the grain growth process of nanocrystal materials both diffusion and surface reaction are important [29]. They suggested that the model for the simulation of the grain growth kinetics of nanocrystal materials should take into account both diffusion and surface reactions. In the model, the rate constant k was expressed as:

$$\begin{aligned}\frac{1}{k} &= \frac{\delta}{k_{\mathrm{D}}} + \frac{1-\delta}{k_{\mathrm{A}}} \\ &= \frac{\delta}{\exp\left(-\frac{Q_{\mathrm{D}}}{RT}\right)} + \frac{1-\delta}{\exp\left(-\frac{Q_{\mathrm{A}}}{RT}\right)} \\ &= \delta\exp\left(\frac{Q_{\mathrm{D}}}{RT}\right) + (1-\delta)\exp\left(\frac{Q_{\mathrm{A}}}{RT}\right)\end{aligned} \tag{6}$$

where δ is the partition coefficient of the diffusion. When δ=1, the grain growth is controlled by diffusion; when δ=0, the grain growth is controlled by surface reactions. For the grain growth of nanocrystal, δ is

DOI:10.1088/1674-0068/21/03/295-300

between 0 and 1. k_D and k_A are the rate constants of diffusion and surface reactions respectively. Q_D and Q_A are the activation energy of diffusion and surface reactions respectively. Since D_0 is generally much smaller that D, from Eq.(4), Eq.(7) can be obtained.

$$\begin{aligned} 1/D &= k^{-1/n}t^{-1/n} \\ &= \left[\delta \exp\left(\frac{Q_D}{RT}\right) + (1-\delta)\exp\left(\frac{Q_A}{RT}\right)\right]^{1/n} t^{-1/n} \end{aligned} \tag{7}$$

According to [29], by defining a combined activation energy,

$$\bar{Q}_{DA} = \lambda Q_D + (1-\lambda)Q_A \tag{8}$$

The relationship between D and T can be expressed by Eq.(9) for a fixed calcination duration at high temperatures.

$$\begin{aligned} \frac{1}{D} &\approx \left(1 + \frac{\bar{Q}_{DA}}{RT}\right)^{1/n} t^{-1/n} \\ &= \left(1 + \frac{\bar{Q}_{DA}}{nRT}\right) t^{-1/n} \\ &= t^{-1/n} + t^{-1/n}\frac{\bar{Q}_{DA}}{nRT} \\ &= A_1 + \frac{B_1}{T} \end{aligned} \tag{9}$$

Accordingly, the relationship of D and T in the conventional model can be expressed as:

$$\ln D = A_2 + \frac{B_2}{T} \tag{10}$$

Using the experimental data obtained at calcination temperatures from 700 °C to 1200 °C, and Eq.(10) and Eq.(11), simulations of the grain growth kinetics were performed. The results are shown in Table I and Fig.8.

For linear regression with conventional model, the relative error is in the range of 0.0034-0.0768, the correlation coefficient is 0.9784, the standard deviation is 0.0681. For linear regression with isothermal model, the relative error is in the range of 0.0011-0.0476, the correlation coefficient is 0.9953, the standard deviation is 0.009. It is apparent that the isothermal model gives better simulation results than the conventional model does, implying that the grain growth model for the nanocrystal materials proposed by Qu and Song [29] is more close to practical grain growth process.

Using the above obtained value of n (n=7) and Eq.(9), the mixed activation energy can be estimated, $\bar{Q}_{DA}$=27.23 kJ/mol.

TABLE I Simulation results using the conventional model and the new isothermal model

T/°C	D_{exp}/nm	Isothermal model		Conventional model	
		D_{calc}/nm	R^a	D_{calc}/nm	R^a
700	23.6	23.06	0.0238	22.09	0.0639
800	27	27.44	0.0163	27.86	0.0318
900	31.4	32.21	0.0258	33.36	0.0624
1000	36.4	37.40	0.0274	38.53	0.0585
1100	43.5	43.45	0.0011	43.35	0.0034
1200	51.8	49.33	0.0476	47.82	0.0768

[a] Relative error.

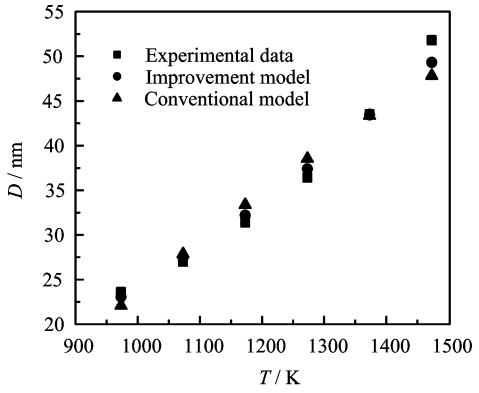

FIG. 8 Comparision of the experimental and the simulated D values.

IV. CONCLUSION

$BaTiO_3$ nanocrystals were obtained using sol-gel method. The results of TG and DSC analyses indicate that decomposition of the xerogel proceeds via five stages. The XRD results of the $BaTiO_3$ nanocrystals indicate that calcination temperature and duration do not have a significant influence on the lattice constant. With increasing calcination temperature or duration, lattice distortion of $BaTiO_3$ nanocrystal decreases, while the grain size enlarges. The grain growth kinetics were simulated with a conventional model which takes into account only diffusion and with an isothermal model which takes into account both diffusion and surface reactions during the grain growth process. With the conventional model, a pre-exponential factor of 7 and an activation energy of 75.49 kJ/mol for the rate constant of k was obtained. With the isothermal model, a combined activation energy of 27.23 kJ/mol was obtained. The simulation results indicate that the isothermal model is superior to the conventional model in matching the experimental data. This means that the surface reactions during the grain growth process of the nano $BaTiO_3$ also play an important role.

[1] Y. Sakabe, Y. Yamashita, and H. Yamamoto, J. Eur. Ceram. Soc. **25**, 2739 (2005).
[2] Reynolds III and G. Thomas, Am. Ceram. Soc. Bull. **80**, 29 (2001).
[3] Y. Ch. Lee, Ch. T. Lee, S. Wang, and F. S. Shieu, Mater. Chem. Phys. **100**, 355 (2006).

DOI:10.1088/1674-0068/21/03/295-300

[4] Y. Luo, X. Y. Liu, and X. Q. Li, Solid State Ionics **117**, 1543 (2006).
[5] D. H. Kang, K. W. Kim, and S. Y. Lee, Mater. Chem. Phys. **90**, 411 (2005).
[6] Y. X. Hu, D. X. Zhou, D. L. Zhang, and W. Z. Lu, Sens. Actuators A Phys. **88**, 67 (2001).
[7] B. M. Kulwicki, J. Phys. Chem. Solids **45**, 1015 (1984).
[8] C. Gómez-Yáñez, E. Cruz-Aquino, and J. J. Cruz-Rivera, J. Alloys Compd. **434-435**, 806 (2007).
[9] A. Y. Fasasi, F. A. Balogun, and M. K. Fasasi, Sens. Actuators A Phys. **135**, 598 (2007).
[10] W. D. Wu, Y. J. He, and F. Wang, J. Cryst. Growth. **54**, 1231 (2006).
[11] K. Suzuki and K. Kijima, Vacuum **80**, 519 (2006).
[12] H. S. Potdar, B. D. Deshpande, and S. K. Date, Mater. Chem. Phys. **58**, 295 (1999).
[13] C. Marin, M. Odile, and L. Philip, J. Eur. Ceram. Soc. **32**, 3241 (2006).
[14] T. Yan, X. L. Liu, and N. R. Wang, J. Cryst. Growth. **281**, 669 (2005).
[15] C. P. Nimai, S. Sang, and Y. A. Bok, Mater. Res. Bull. **42**, 497 (2007).
[16] S. G. Kwon, K. Choi, and B. L. Kim, Mater. Lett. **60**, 979 (2006).
[17] P. Durán, F. Capel, and J. Tartaj, Solid State Ionics **141-142**, 529 (2001).
[18] L. Q. Wang, L. Liu, and D. F. Xue, J. Alloys Compd. **440**, 78 (2007).
[19] Y. Q. Huang, J. R. Lin, and H. Y. Du, Mater. Lett. **60**, 3818 (2006).
[20] J. H. Cho and M. Kuwabara, J. Eur. Ceram. Soc. **24**, 2959 (2004).
[21] B. Lee and J. P. Zhang, Thin Solid Films **388**, 107 (2001).
[22] M. B. Park, C. D. Kim, and S. K. Lee, Appl. Surf. Sci. **190**, 416 (2002).
[23] M. B. Park, S. J. Hwang, and N. H. Cho, Mater. Sci. Eng. **99**, 155 (2003).
[24] J. E. Kim, C. H. Song, and H. W. Park, Mater. Sci. Eng. A **449-451**, 299 (2007).
[25] A. Kundu, S. Anand, and H. C. Verma, Adv. Powder Technol. **132**, 131 (2003).
[26] P. Vasili, S. W. Chan, and F. Zhang, Solid State Commun. **123**, 295 (2002).
[27] L. Gao, Y. X. Qu, X. L. Song, and Y. R. Ma, J. Chin. Ceram. Soc. **33**, 1157 (2005).
[28] M. Hillert, Acta. Metal. **13**, 227 (1966).
[29] Y. X. Qu and X. L. Song, J. Chem. Ind. Eng. **55**, 1206 (2004).

DOI:10.1088/1674-0068/21/03/295-300